# Characterisation and environmental application of an Australian natural zeolite for basic dye removal from aqueous solution

Shaobin Wang [a],*, Z.H. Zhu [b]

[a] *Department of Chemical Engineering, Curtin University of Technology, G.P.O. Box U1987, Perth, WA 6845, Australia*
[b] *ARC Centre for Functional Nanomaterials, University of Queensland, Brisbane 4072, Australia*

## Abstract

An Australian natural zeolite was collected, characterised and employed for basic dye adsorption in aqueous solution. The natural zeolite is mainly composed of clinoptiloite, quartz and mordenite and has cation-exchange capacity of 120 meq/100 g. The natural zeolite presents higher adsorption capacity for methylene blue than rhodamine B with the maximal adsorption capacity of $2.8 \times 10^{-5}$ and $7.9 \times 10^{-5}$ mol/g at 50 °C for rhodamine B and methylene blue, respectively. Kinetic studies indicated that the adsorption followed the pseudo second-order kinetics and could be described as two-stage diffusion process. The adsorption isotherm could be fitted by the Langmuir and Freundlich models. Thermodynamic calculations showed that the adsorption is endothermic process with $\Delta H^\circ$ at 2.0 and 8.7 kJ/mol for rhodamine B and methylene blue. It has also found that the regenerated zeolites by high-temperature calcination and Fenton oxidation showed similar adsorption capacity but lower than the fresh sample. Only 60% capacity could be recovered by the two regeneration techniques.
© 2006 Elsevier B.V. All rights reserved.

*Keywords:* Natural zeolite; Dye removal; Wastewater treatment; Kinetics; Isotherm

## 1. Introduction

Many industries such as textile and printing use dyes and pigments and thus produce highly coloured waste effluents. Disposal of these wastes into waters causes environmental problems. Various methods for dye and colour removal, such as aerobic and anaerobic microbial degradation, coagulation and chemical oxidation, membrane separation process, electrochemical, filtration, softening and reverse osmosis have been proposed from time to time [1]. However, all of the methods suffered from one or another limitation and none of the processes described above were successful in removing colour from wastewater completely. Adsorption is probably the simplest process for dye removal. Currently, activated carbon is believed to be the most effective adsorbent. However, high cost in production and regeneration make it uneconomical [2].

Natural zeolite is an abundant resource of aluminosilicates available all over the world. Natural zeolite usually has high cation exchange capacity. There are many possible uses of the natural sedimentary zeolites such as for building stone, cement pozzolan, lightweight aggregate, oil spill cleanup, paper filler, desiccants and for gas and liquid separations. One of the most significant commercial applications of natural zeolites is the removal of heavy metal ions from wastewater [3–7]. In addition, natural zeolites have also been used for adsorption of ammonium [8–10] and organics [11,12] in water. However, few investigations have been conducted in dye removal using natural zeolite [13,14]. Some investigations have been reported using organic-zeolite composites for dye removal [13,15,16]. Metes et al. [14] also investigated several synthetic zeolites for cleaning printing ink wastewater and found that adsorption is independent of pore structure. ZSM-5 and $NH_4$-beta are effective while other zeolites studied showed lower efficiency. In this paper, we report an investigation using an Australian natural zeolite for dye removal. We investigated the kinetics, equilibrium isotherm and thermodynamics as well as physical and chemical methods for regeneration of the spent natural zeolite in adsorption of basic dyes.

* Corresponding author.
  *E-mail address:* wangshao@vesta.curtin.edu.au (S. Wang).

Table 1
Physicochemical properties of natural zeolite

| Chemical compound | % |
| --- | --- |
| $SiO_2$ | 68.26 |
| $Al_2O_3$ | 12.99 |
| $Fe_2O_3$ | 1.37 |
| CaO | 2.09 |
| MgO | 0.83 |
| $K_2O$ | 4.11 |
| $TiO_2$ | 0.23 |
| $Na_2O$ | 0.64 |
| MnO | 0.06 |
| $P_2O_5$ | 0.06 |
| LOI | 8.87 |
| CEC | 120 meq/100 g |
| Particle size | <75 μm |
| Molecular channel size | 7.9 Å × 3.5 Å |
| $S_{BET}$ | 16.0 m$^2$/g |
| Pore volume | 0.039 cm$^3$/g |
| pH | 8.5 |

## 2. Materials and adsorption test

### 2.1. Adsorbent and dyes

A natural zeolite was obtained from Zeolite Australia Ltd. Its physicochemical properties are presented in Table 1. XRF measurement shows that the chemical compositions of the natural zeolite are $SiO_2$, $Al_2O_3$, CaO, $K_2O$ and $Fe_2O_3$. Most of natural zeolite contains large amount of clinoptilolite, which has a three-dimensional crystal structure. It is known that natural zeolite usually has some ion exchangeable cations such as Na, K, Ca and Mg in channels. Such cations give a high cation exchange capability to zeolite, hence it can be exchanged with organic such as cationic dyes and inorganic cations like heavy metals. Thus, two basic dyes were chosen for investigation, methylene blue (MB) and rhodamine B (RB), which were obtained from AJAX Chemicals. Their chemical structures are presented in Fig. 1. A stock solution with concentration at $10^{-4}$ M was prepared and the solutions for adsorption tests were prepared from the stock solution to the desired concentration.

### 2.2. Characterisation techniques

The phases of the natural zeolite were determined by XRD analyses with an automated Rigaku miniflex diffractometer using Co Kα radiation at 40 kV and 40 mA over the range (2θ) of 5–80°.

The surface area ($S_{BET}$), total pore volume and pore size distribution were determined by $N_2$ adsorption isotherm with relationship between $N_2$ adsorbed volume at standard conditions (V) and the partial pressure ($p/p^0$) under $-196\,^\circ$C using Autosorb (Quantachrome Corp.). Before adsorption, the samples were degassed at $200\,^\circ$C for 4 h, prior to the adsorption experiments. The BET surface area was obtained by five points at $p/p^0$ between 0.05 and 0.20 applying the BET equation to the adsorption data. The total pore volume was calculated at $p/p^0 = 0.95$. The pore size distribution was obtained using BJH method [17].

The pH of natural zeolite was measured as follows: 0.1 g of samples were mixed with 10 ml of distilled water and shaken for 24 h at $30\,^\circ$C. After filtration, the pH of solution was determined by a pH meter (Radiometer PHM250 ion Analyser).

### 2.3. Sorption method

Sorption studies were performed by batch technique to obtain rate and equilibrium data. The batch technique was selected because of its simplicity. For kinetic and isotherm studies, a series of 250 ml bottles were employed. Each bottle was filled with 200 ml of dye solution of varying concentrations ($10^{-6}$ to $10^{-5}$ M) and a known amount of adsorbent. The sorption studies were carried out at different temperatures, 30 and $50\,^\circ$C. 0.05 g of absorbents was added to the bottles, which were agitated intermittently for the desired time periods. After this period, the solution was spectroscopically analysed using Spectronic 20 Genesys Spectrophotometer (Spectronic Instrument) at the corresponding $\lambda_{max} = 665$ and 556 nm for methylene blue and rhodamine B for the concentration of dye remaining in solution. The dye concentration retained in the adsorbent phase was calculated according to

$$Q_e = \frac{(C_0 - C_e)V}{W} \tag{1}$$

where $C_0$ and $C_e$ are the initial and equilibrium concentrations (M), respectively, of dye in solution; V the volume (L); and W is the weight (g) of the adsorbent.

### 2.4. Physical and chemical regeneration of spent natural zeolite

The used natural zeolite was regenerated by two methods, physical treatment via calcination and chemical treatment by Fenton oxidation. In physical treatment, the used zeolite was
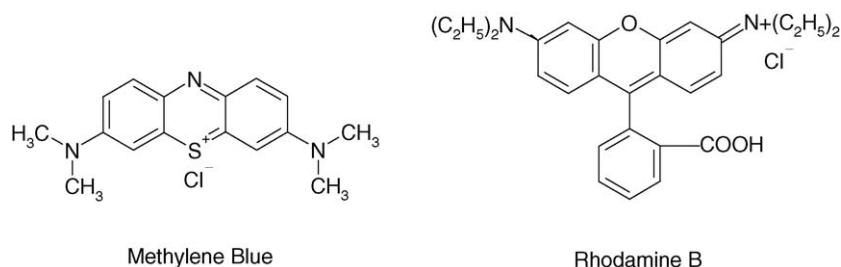


Fig. 1. Chemical structure of dyes.

calcined at high temperature, keeping at 550 °C for 5 h. For Fenton oxidation, the used adsorbents were mixed with 0.01 M $FeSO_4$ and 3% $H_2O_2$ solution for 24 h at pH around 6 and the regeneration was performed two times. Then the solid samples were filtered, washed and dried for adsorption tests again. It is known that Fenton oxidation occurs at acid conditions and the optimal pH is 3, at which the reaction rate is fast. In this work, the regeneration was conducted at pH 6 to avoid any effect of acid treatment, which could change the surface properties of solids.

## 3. Results and discussion

### 3.1. Characterisation of natural zeolite

Table 1 presents some properties of the natural zeolite. As shown, the cation exchange capacity is 120 meq/100 g. The solid slurry pH is greater than 7, indicating that the zeolite shows negative charge in aqueous solution. XRD measurement also shows that the natural zeolite is mainly composed of clinoptilolite, quartz and mordenite. $N_2$ adsorption isotherm and pore size distribution are presented in Fig. 2. The BET surface area and total pore volume were given in Table 1. As seen that BET surface area and pore volume are not higher, only 16 $m^2$/g and

0.040 $cm^3$/g. For natural zeolite the pore size distribution only shows one peak centred at 40 Å, suggesting a very narrow pore size.

### 3.2. Dynamic adsorption and kinetics

Fig. 3 illustrates the dynamic adsorption of methylene blue and rhodamine B on natural zeolite at different temperatures. It is seen that two dyes exhibit different adsorption rates. The adsorption of RB on zeolite will be faster to reach equilibrium at around 50 h while it will take a longer time (200 h) to arrive at the equilibrium for MB. At each temperature, zeolite exhibits higher adsorption for MB than RB due to its smaller molecular size than RB, which can be seen from Fig. 1. As seen from Fig. 3 that adsorption temperature will influence the adsorption capacity. For two dyes, the adsorption at 50 °C is higher than that at 30 °C, suggesting the endothermic characteristic of the adsorption. For the adsorption, the process is usually a diffusion process with endothermic property. A higher temperature can result in an increase in the mobility of the dye ions and their energy to undergo an interaction with active sites at the surface of adsorbents. Furthermore, increasing temperature may produce a swelling effect within the internal structure of the zeolite enabling large dyes to penetrate further into the pores [2].
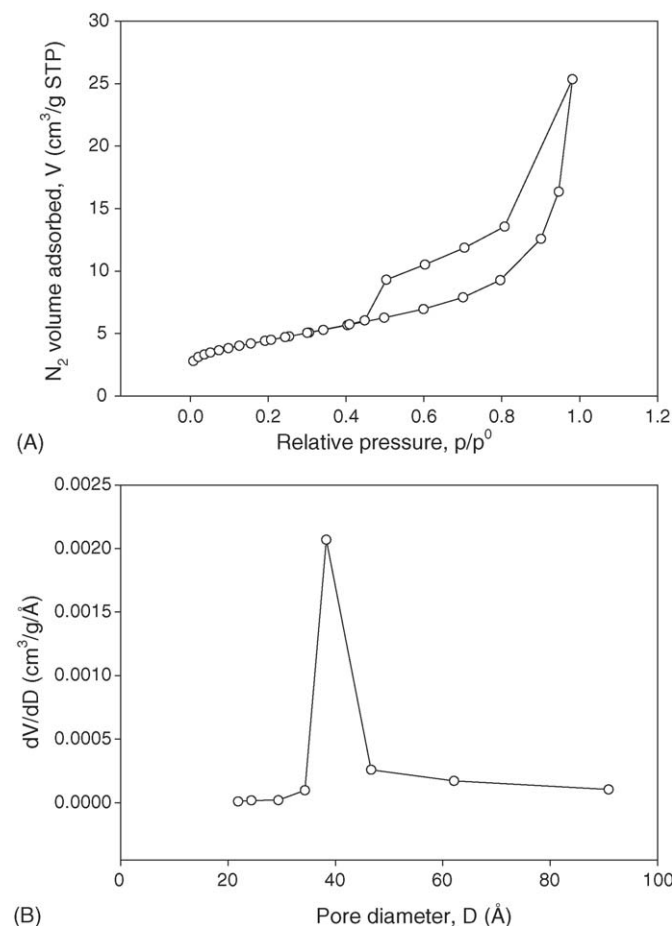


Fig. 2. $N_2$ adsorption isotherm and pore size distribution of natural zeolite: (A) adsorption isotherm and (B) pore size distribution.
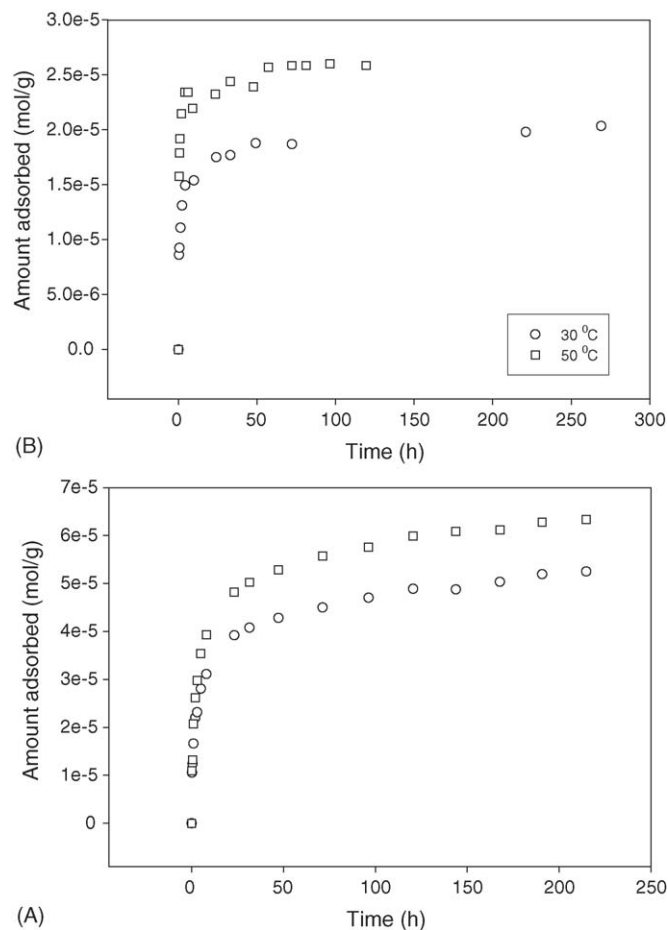


Fig. 3. Dynamic adsorption of MB and RB on natural zeolite: (A) MB and (B) RB.

It is known that ionic dyes upon dissolution release coloured dye anions/cations into solution. The adsorption of these charged dye groups onto the adsorbent surface is primarily influenced by the surface charge on the adsorbent. In water, basic dyes produce an intense molecular cation ($C^+$) and reduced ions ($CH^+$). As zeolite particles exhibit negative charge in water, electrostatic interaction will favour the adsorption of basic dyes on zeolite. In addition, the pore size could also play a role in adsorption. For the same adsorbent, large size molecules will not easily penetrated into the inner pores of the adsorbent, resulting in lower adsorption capacity.

The kinetics of adsorption can be described using several models. A simple kinetic analysis of adsorption is the pseudo first-order equation

$$\frac{dq_t}{dt} = k_1(q_e - q_t) \tag{2}$$

where $k_1$ is the rate constant of pseudo first-order adsorption and $q_e$ denotes the amount of adsorption at equilibrium. After definite integration by applying the initial conditions $q_t = 0$ at $t = 0$ and $q_t = q_t$ at $t = t$, Eq. (2) becomes

$$\ln(q_e - q_t) = \ln(q_e) - k_1 t \tag{3}$$

The above linear equation based on $\ln(q_e - q_t)$ and $t$ can usually be used to estimate the equilibrium adsorption $q_e$ (intercept) and rate constant $k_1$ (slope). If the calculated $q_e$ from intercept is equal to the experimental $q_e$, it would suggest the adsorption following the first-order kinetics [18].

A pseudo second-order equation based on adsorption equilibrium capacity may be expressed in the form

$$\frac{dq_t}{dt} = k_2(q_e - q_t)^2 \tag{4}$$

where $k_2$ is the rate constant of pseudo second-order adsorption. Integrating and applying the initial conditions, we have a linear form as

$$\frac{t}{q_t} = \frac{1}{k_2 q_e^2} + \frac{1}{q_e} t \tag{5}$$

In addition, another simplified model, intraparticle diffusion model, is also tested. The initial rate of the intraparticle diffusion is the following:

$$q_t = k_p(t^{1/2}) \tag{6}$$

where $k_p$ is the intraparticle diffusion rate constant.

Figs. 4–5 present the linear forms of the first-order and second-order kinetics of two dyes adsorbed on zeolite and the calculated kinetic parameters are given in Table 2. As seen, the first-order kinetics curve does not show a straight line and two sections can be clearly identified. The correlation coefficients are also much lower (0.83–0.94). The calculated $q_e$ deviates much from the experimental value, which indicates the inapplicable to the first-order kinetics. On the contrary, the second-order kinetic curves show much better correlation coefficients, close to 0.999 in all cases. Also the calculated $q_e$ is much close to the experimental value. Thus, it is derived that the adsorption of basic
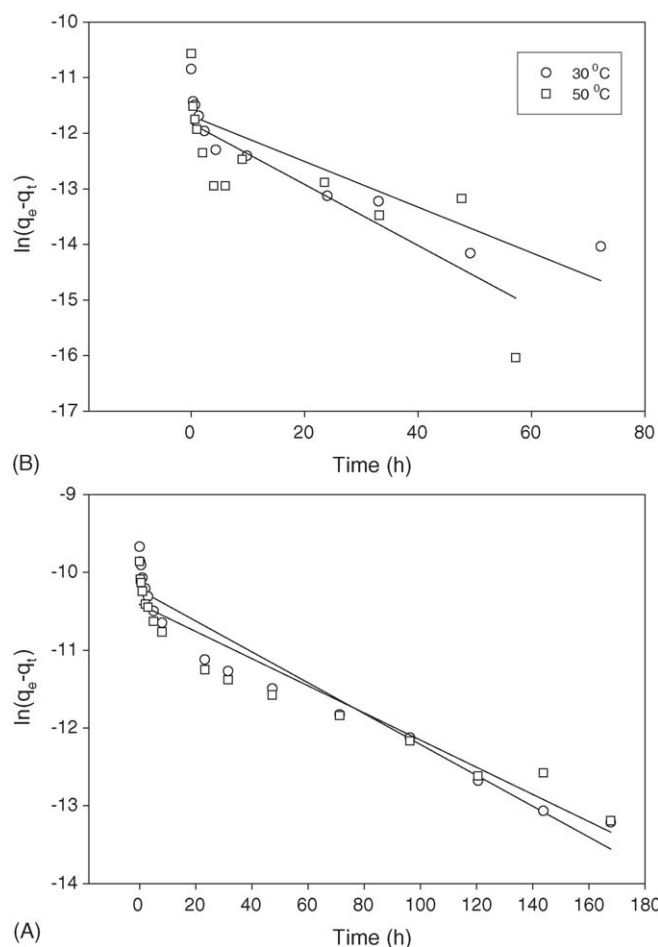


Fig. 4. The first-order kinetics of MB and RB adsorption on natural zeolite: (A) MB and (B) RB.

dyes on natural zeolite follows the pseudo second-order kinetics. Comparing the adsorption equilibrium, it is seen that the value at 50 °C are higher than 30 °C, conformed to the experimental data.

Fig. 6 shows the diffusion modelling on kinetics of dye adsorption on natural zeolite. One can see that the adsorption is in two stages. The first one is attributed to external surface adsorption and the second one should be intraparticle diffusion process. Previous studies have showed similar results that a multi-step is involved in the adsorption process of dye on several solid adsorbents [19–21].

### 3.3. Adsorption equilibrium

The equilibrium adsorption isotherm is fundamental in describing the interactive behaviour between solutes and adsorbent, and is important in the design of adsorption system. Fig. 7 shows the adsorption isotherms of MB and RB at different temperatures. As shown, the adsorption increases with the increasing equilibrium concentration and approaches to equilibrium at higher concentration. Higher temperature results in higher adsorption capacity. The adsorption capacities for MB at 30 and 50 °C can be estimated as $5.5 \times 10^{-5}$ and $6.3 \times 10^{-5}$ mol/g at equilibrium concentration of $2.0 \times 10^{-5}$ M,

Table 2
Kinetic parameters of dye adsorption on natural zeolite

| Dyes | Temperature (°C) | Experimental | First-order kinetics | | | Second-order kinetics | | |
|------|------------------|--------------|----------------------|------|-------|-----------------------|------|-------|
| | | $q_e$ (mol/g) | $q_e$ (mol/g) | $k_1$ (1/h) | $R^2$ | $q_e$ (mol/g) | $k_2$ (mol/g h) | $R^2$ |
| RB | 30 | $1.95 \times 10^{-5}$ | $8.40 \times 10^{-6}$ | 0.041 | 0.834 | $2.03 \times 10^{-5}$ | $1.92 \times 10^{4}$ | 0.999 |
| | 50 | $2.58 \times 10^{-5}$ | $6.51 \times 10^{-6}$ | 0.040 | 0.826 | $2.60 \times 10^{-5}$ | $3.58 \times 10^{4}$ | 0.999 |
| MB | 30 | $5.22 \times 10^{-5}$ | $3.01 \times 10^{-5}$ | 0.0174 | 0.922 | $5.22 \times 10^{-5}$ | $3.48 \times 10^{3}$ | 0.997 |
| | 50 | $6.30 \times 10^{-5}$ | $3.61 \times 10^{-5}$ | 0.0198 | 0.936 | $6.34 \times 10^{-5}$ | $3.13 \times 10^{4}$ | 0.998 |

respectively, while the adsorption capacities for RB at 30 and 50 °C are $2.0 \times 10^{-5}$ and $2.5 \times 10^{-5}$ mol/g at equilibrium concentration of $1.0 \times 10^{-5}$ M.

To simulate the adsorption isotherm, two models are commonly used, the Langmuir and Freundlich isotherms. The well-known expression of the Langmuir model is

$$q_e = \frac{K_L q_{max} C_e}{1 + K_L C_e} \quad (7)$$

where $q_e$ is the equilibrium dye concentration on adsorbent (mol/g), $C_e$ the equilibrium dye concentration in solution (mol/l), $q_{max}$ the monolayer capacity of the adsorbent (mol/g) and $K_L$ is the Langmuir adsorption constant (l/mol) which relates to the adsorption energy. The Langmuir equation is applicable to homogeneous sorption, where the sorption of each sorbate molecule onto the surface has equal sorption activation energy.

On the other hand, the Freundlich equation is

$$q_e = K_F C_e^{1/n} \quad (8)$$

where $q_e$ is the equilibrium dye concentration on adsorbent (mol/g), $C_e$ the equilibrium dye concentration in solution (mol/l) and $K_F$ (l/g) and $n$ are the Freundlich constants characteristic of the system, indicators of adsorption capacity and adsorption intensity, respectively. The Freundlich equation is employed to describe heterogeneous systems and reversible adsorption and is not restricted to the formation of monolayers.
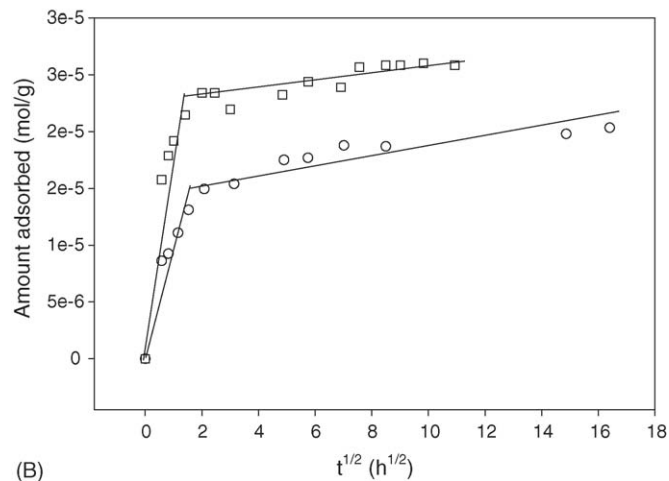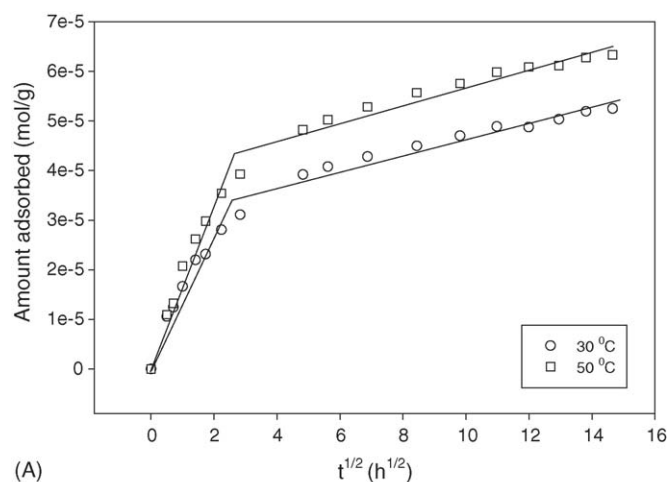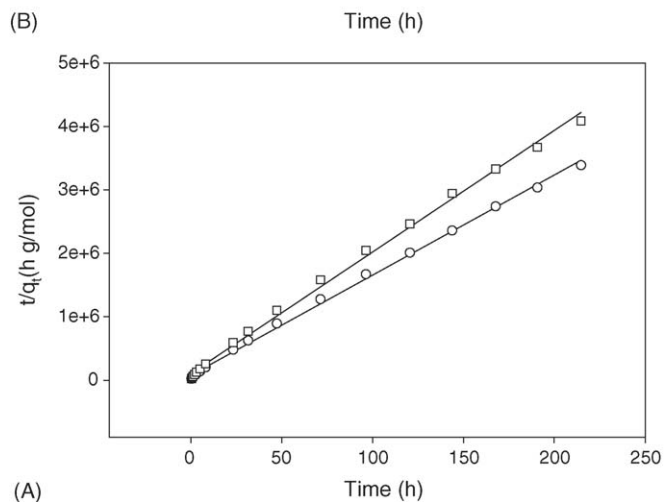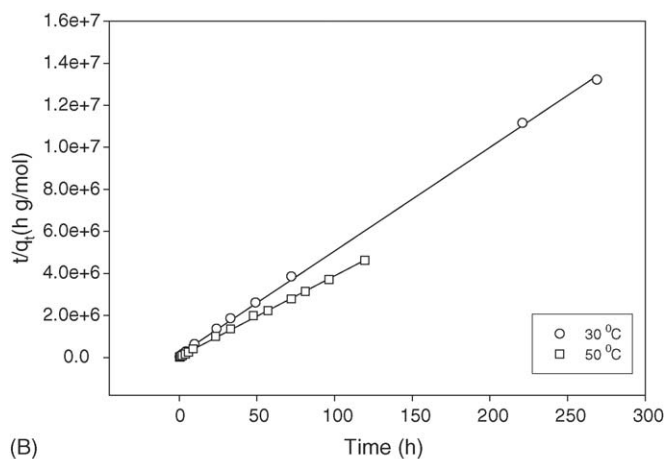


Fig. 5. The second-order kinetics of MB and RB adsorption on natural zeolite: (A) MB and (B) RB.



Fig. 6. Intraparticle diffusion modelling of MB and RB adsorption on natural zeolite: (A) MB and (B) RB.
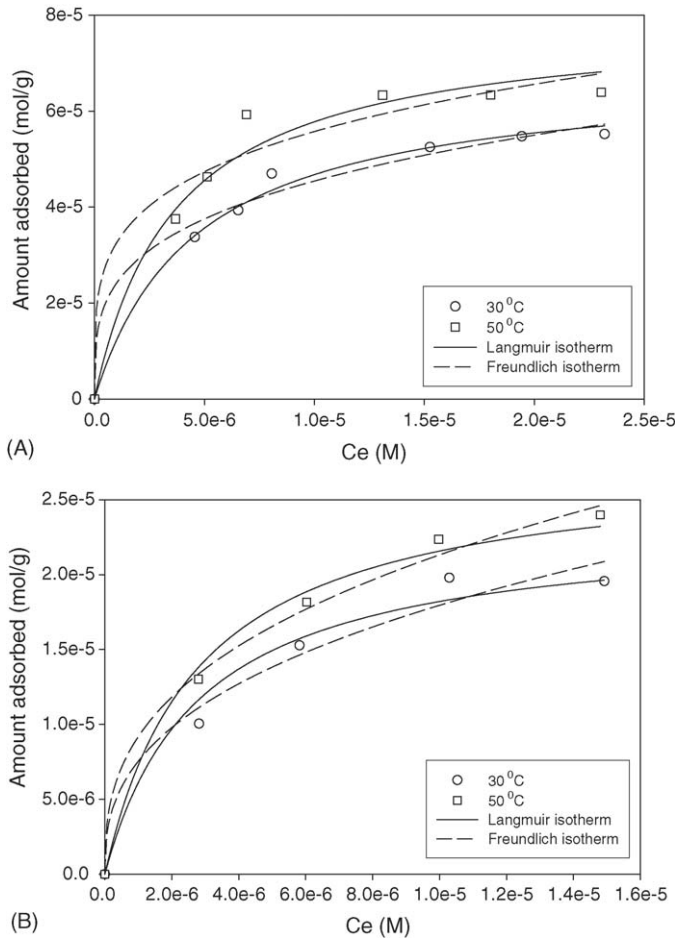
(A)

(B)

Fig. 7. Adsorption isotherm of MB and RB on natural zeolite at different temperatures: (A) MB and (B) RB.

Table 4
Thermodynamic parameters of dye adsorption on natural zeolite

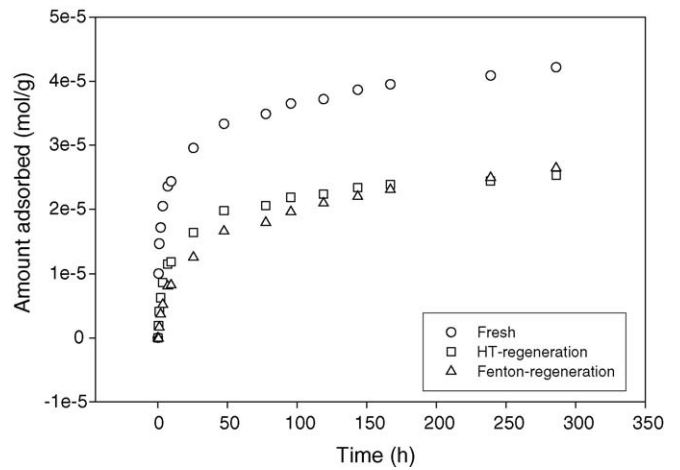| Dyes | Temperature (°C) | $\Delta G^\circ$ (kJ/mol) | $\Delta H^\circ$ (kJ/mol) | $\Delta S^\circ$ (J/mol K) |
|------|------------------|---------------------------|---------------------------|----------------------------|
| RB | 30 | −32.1 | 2.0 | 112.4 |
| | 50 | −34.3 | | |
| MB | 30 | −31.0 | 8.7 | 127.6 |
| | 50 | −31.5 | | |



Fig. 8. Comparison of natural zeolite and the regenerated forms for MB adsorption at 30 °C.

$$\Delta S^\circ = \frac{\Delta H^\circ - \Delta G^\circ}{T} \qquad (11)$$

As seen that the adsorption process is spontaneous with the negative values of $\Delta G^\circ$. The standard enthalpy change ($\Delta H^\circ$) for the adsorption of two dyes on natural zeolite is positive indicating that the process is endothermic in nature. The positive value of $\Delta S^\circ$ shows increased disorder at the solid–solution interface during the adsorption of dyes. The adsorption increases randomness at the solid/solution interface with some structural changes in the adsorbate and adsorbent and an affinity of the adsorbent.

### 3.4. Regeneration of natural zeolite

Fig. 8 shows a comparison of dynamic adsorption of fresh zeolite and regenerated zeolites. As shown, the regenerated zeolite either from high-temperature calcination or Fenton oxidation shows similar adsorption behaviour and the adsorption capacity from physical treatment is slight higher than the one of chemical treatment. The two regenerated zeolites presented lower

The non-linear forms of the two isotherms to the experimental data are illustrated in Fig. 7. Table 3 lists the calculated results. The fits for two isotherms are quite similar. The correlation coefficients for two models are all greater than 0.95, indicating that the two models fit the experimental well.

Based on the adsorption constant $K_L$ in the Langmuir isotherm, thermodynamic parameters, i.e., free energy ($\Delta G^\circ$), enthalpy ($\Delta H^\circ$) and entropy ($\Delta S^\circ$), changes were also calculated using Eqs. (9–11) and are given in Table 4:

$$\Delta G^\circ = -RT \ln K_L \qquad (9)$$

$$\Delta H^\circ = -R \left( \frac{T_2 T_1}{T_2 - T_1} \right) \ln \frac{K_{L1}}{K_{L2}} \qquad (10)$$

Table 3
Parameters for adsorption isotherms on natural zeolite

| Dyes | Temperature (°C) | Langmuir isotherm | | | Freundlich isotherm | | |
|------|------------------|-------------------|-----------------|-------|---------------------|-------|-------|
| | | $q_{max}$ (mol/g) | $K_L$ (l/mol) | $R^2$ | $K$ (mol/g) | $1/n$ | $R^2$ |
| RB | 30 | $2.12 \times 10^{-5}$ | $3.41 \times 10^5$ | 0.974 | $6.21 \times 10^{-4}$ | 0.318 | 0.952 |
| | 50 | $2.76 \times 10^{-5}$ | $3.58 \times 10^5$ | 0.992 | $1.44 \times 10^{-3}$ | 0.366 | 0.996 |
| MB | 30 | $6.81 \times 10^{-5}$ | $2.19 \times 10^5$ | 0.993 | $1.08 \times 10^{-3}$ | 0.276 | 0.986 |
| | 50 | $7.91 \times 10^{-5}$ | $2.71 \times 10^5$ | 0.973 | $8.33 \times 10^{-4}$ | 0.235 | 0.956 |

adsorption capacity than the fresh sample and the reduction in adsorption is more than 40%. High-temperature calcination will decompose the organic dyes on surface or in pores of solid to carbon and then oxidised to carbon oxides in air. However, high-temperature calcination can also change the surface function groups and cause the pore collapse, resulting in lower surface area and pore volume and leading to lower adsorption capacity. Fenton oxidation can destruct the organics by hydroxyl radicals but it will produce adsorption of Fe ions in zeolite during the process thus reducing the adsorption for other cation ions such as dyes on zeolite.

## 4. Conclusion

A natural zeolite has been tested for adsorption of basic dyes, methylene blue and rhodamine B. It is found that zeolite exhibits higher MB adsorption than RB due to the difference in molecular size. For methylene blue, the adsorption capacities are $6.8 \times 10^{-5}$ and $7.9 \times 10^{-5}$ mol/g at 30 and 50 °C, respectively. In contrast, the adsorption capacities of rhodamine B are $2.1 \times 10^{-5}$ and $2.8 \times 10^{-5}$ mol/g at 30 and 50 °C, respectively. Thermodynamic and kinetic calculations indicate that the adsorption is endothermic reaction with two-step diffusion process. The adsorption enthalpies on RB and MB are 2.0 and 8.7 kJ/mol, respectively. The kinetics of adsorption will be better described by the pseudo second-order model. The Langmuir and Freundlich models can also describe well the adsorption isotherm. Regeneration of natural zeolite by high-temperature calcination and Fenton chemical oxidation can only restore 60% of adsorption capacity.

## References

[1] T. Robinson, G. McMullan, R. Marchant, P. Nigam, Remediation of dyes in textile effluent: a critical review on current treatment technologies with a proposed alternative, Bioresour. Technol. 77 (2001) 247–255.

[2] S.B. Wang, Y. Boyjoo, A. Choueib, Z.H. Zhu, Removal of dyes from aqueous solution using fly ash and red mud, Water Res. 39 (2005) 129–138.

[3] S.M. Dal Bosco, R.S. Jimenez, W.A. Carvalho, Removal of toxic metals from wastewater by Brazilian natural scolecite, J. Colloid. Interface Sci. 281 (2005) 424–431.

[4] R.S. Jimenez, S.M. Dal Bosco, W.A. Carvalho, Heavy metals removal from wastewater by the natural zeolite scolecite—temperature and pH influence in single-metal solutions, Quim Nova 27 (2004) 734–738.

[5] M. Panayotova, B. Velikov, Kinetics of heavy metal ions removal by use of natural zeolite, J. Environ. Sci. Health A 37 (2002) 139–147.

[6] M. Trgo, J. Peric, Interaction of the zeolitic tuff with Zn-containing simulated pollutant solutions, J. Colloid. Interface Sci. 260 (2003) 166–175.

[7] A.E. Turkman, S. Aslan, I. Ege, Treatment of metal containing wastewaters by natural zeolites, Fresenius Environ. Bull. 13 (2004) 574–580.

[8] S. Aiyuk, H. Xu, A. van Haandel, W. Verstraete, Removal of ammonium nitrogen from pretreated domestic sewage using a natural ion exchanger, Environ. Technol. 25 (2004) 1321–1330.

[9] A.H. Englert, J. Rubio, Characterization and environmental application of a Chilean natural zeolite, Int. J. Miner. Process. 75 (2005) 21–29.

[10] S. Komarowski, Q. Yu, Ammonium ion removal from wastewater using Australian natural zeolite: Batch equilibrium and kinetic studies, Environ. Technol. 18 (1997) 1085–1097.

[11] S. Syamsiah, I.S. Hadi, Adsorption cycles and effect of microbial population on phenol removal using natural zeolit, Sep. Purif. Technol. 34 (2004) 125–133.

[12] Y.C. Chung, D.H. Son, D.H. Ahn, Nitrogen and organics removal from industrial wastewater using natural zeolite media, Water Sci. Technol. 42 (2000) 127–134.

[13] B. Armagan, M. Turan, O. Ozdemir, M.S. Celik, Color removal of reactive dyes from water by clinoptilolite, J. Environ. Sci. Health A 39 (2004) 1251–1261.

[14] A. Metes, D. Kovacevic, D. Vujevic, S. Papic, The role of zeolites in wastewater treatment of printing inks, Water Res. 38 (2004) 3373–3381.

[15] B. Armagan, O. Ozdemir, M. Turan, M.S. Celik, The removal of reactive azo dyes by natural and modified zeolites, J. Chem. Technol. Biot. 78 (2003) 725–732.

[16] D. Balkose, S. Ulutan, F. Ozkan, S. Ulku, U. Kokturk, Flexible poly(vinyl chloride)-zeolite composites for dye adsorption from aqueous solutions, Separ. Sci. Technol. 31 (1996) 1279–1289.

[17] E.P. Barrett, L.G. Joyner, P.P. Halenda, The determination of pore volume and area distributions in porous substances. I. Computations from nitrogen isotherms, J. Am. Chem. Soc. 73 (1951) 373–380.

[18] Y.S. Ho, G. McKay, A comparison of chemisorption kinetic models applied to pollutant removal on various sorbents, Process. Saf. Environ. 76 (1998) 332–340.

[19] K.V. Kumar, V. Ramamurthi, S. Sivanesan, Modeling the mechanism involved during the sorption of methylene blue onto fly ash, J. Colloid. Interface Sci. 284 (2005) 14–21.

[20] Q. Sun, L. Yang, The adsorption of basic dyes from aqueous solution on modified peat-resin particle, Water Res. 37 (2003) 1535–1544.

[21] M. Sankar, G. Sekaran, S. Sadulla, T. Ramasami, Removal of diazo and triphenylmethane dyes from aqueous solutions through an adsorption process, J. Chem. Technol. Biot. 74 (1999) 337–344.